DEM MODELLING OF WEAR IN HIGH SHEAR MIXERS

Matthew D. SINNOTT[1], Sharen J. CUMMINS[1]* and Paul W. CLEARY[1]

[1] CSIRO Data 61, Clayton, Victoria 3169, AUSTRALIA
*Corresponding author, E-mail address: sharen.cummins@csiro.au

ABSTRACT

The handling of particulate materials in industry often involves equipment subject to highly abrasive conditions. Progressive damage to this equipment over time can significantly alter the nature of the interaction between the particulates and the equipment surfaces. This can lead to changes in material transport resulting in reduced or unpredictable process efficiencies, as well as potential safety issues in the case of equipment failure. The ability to predict the lifespan of a piece of equipment and progressive changes to processing during this lifespan is important for many industries including mining, manufacturing, food processing, and pharmaceuticals. This study introduces a numerical model for particulate wearing of a mixer blade in a batch mixing application. We simulate the particulate flow in a cylindrical mixer using the Discrete Element Method (DEM) and collect locally averaged estimates of shear energy absorption on the surface of the rectangular blade. This is used with a mesh modification algorithm to evolve the surface of the mixer blade forward in time. A series of flow simulations and incremental surface modification are used to predict the progressive shape change of the blade.

NOMENCLATURE

C damping coefficient
β factor used to map surface element wear to nodes
F_n normal collisional force (N)
F_t tangential collisional force (N)
F_{te} elastic component of tangential collisional force (N)
v_n normal velocity (m/s)
v_t tangential velocity (m/s)
k_n normal spring stiffness (N/m)
k_t tangential spring stiffness (N/m)
δt timestep duration (s)
t_w sub-simulation duration (s)
Δx particle overlap (m)
dx nodal displacement (m)
μ dynamic friction coefficient
α wear calibration constant (W/m)
S shear power (W)
W wear (m)
m super-quadric shape factor
a,b super-quadric aspect ratio factors

INTRODUCTION

Optimising the performance of a mixer is an issue of great significance in a variety of particle processing technologies common in pharmaceutical, chemical, food, ceramic and metallurgical industries. Inadequate mixing in the product manufacturing process can result in rejection of a poor quality product. In addition, a typical industrial mixing process is very complex in nature involving flows of discrete particles interacting with sophisticated dynamic equipment configurations operating at a wide range of length scales. While experimental studies have provided valuable information on flow kinematics within mixers, these studies are often limited by the analytical techniques used. Numerical simulation techniques such as the Discrete Element Method (DEM) allow for the study of parameters that are difficult to measure or vary experimentally. DEM has been used in several studies to examine dry granular flows in mixers. Cleary and Sinnott (2008) used DEM to assess the mixing characteristics and flow dynamics in various batch and continuous devices. Sinnott and Cleary (2015) considered the effects of particle shape on mixing performance in a bladed high shear mixer and identified specific mechanisms responsible for the mixing. Zhou et. al. (2004) and Remy et. al. (2009) studied the dependence of friction on the particle flow in a cylindrical bladed mixer. Sakar and Wassgren (2009) investigated the influence of fill level and impeller rotation rate in a continuous bladed blender. An important operational parameter that has yet to be numerically simulated (for any mixing device) is the effect of equipment wear on the mixing characteristics. The mechanisms causing wear in a revolving blade mixer were discussed in Jurevicius et al. (2003). Under intensive wear of the mixer elements, the changing surface morphology changes the particle flow patterns as particles become trapped or crushed in newly formed gaps. This can then lead to undesirable effects such as increasing power consumption and decreasing mixing quality. In this paper we present a numerical study on the influence of impeller wear on the mixing performance of bladed mixer. Bladed mixers are common in industry and are used in processes such as wet granulation (Litster, 2003), agitated drying (Lekhal et al. 2003) and tablet press operations (Conway et al. 2005). However to the best of our knowledge, no work has been done in simulating the performance of a bladed mixer as the blade erodes during the mixing process. In this study we extend the work of Sinnott and Cleary (2015) to quantify how different particle size and different clearances between the blade and the floor and walls affect the blade damage.

SIMULATION TECHNIQUE

Discrete Element Method (DEM)

DEM is a numerical technique used to predict the behaviour of collision dominated particle flows. Each particle in the flow is tracked and all collisions between particles and between particles and boundaries are modelled. The particles are allowed to overlap and the extent of overlap is used in conjunction with a contact force law to give instantaneous forces from knowledge of the current positions, orientations, velocities and spins of the particles. In this study the simplest of the force laws, the

linear spring-dashpot model is used. The overlap Δx scaled by the spring constant k provides a repulsive force. The dashpot contributes an inelastic component to the collision. The damping coefficient C is determined from the specified coefficient of restitution for each combination of materials colliding. The spring and dashpot together define the normal force:

$$F_n = -k\Delta x + Cv_n \qquad (1)$$

where v_n is the normal component of the relative velocity at the contact point. The tangential force is composed of an elastic component and an inelastic component. The elastic component, F_{te} is calculated using

$$F_{te}^n = F_{te}^{n-1} + k_t v_t \delta t \qquad (2)$$

where for a given timestep n, F_{te}^n is the elastic component of the tangential force, k_t is the tangential spring stiffness and v_t is the relative tangential surface velocity. The inelastic component is calculated using a dashpot with damping coefficient C. The tangential force is then subject to the sliding Coulomb friction limit to give:

$$F_t = \min\left(\mu F_n, F_{te}^{n-1} + Cv_t\right) \qquad (3)$$

Further details of the implementation are given in Cleary and Sinnott (2008).

In this work, the non-round particle shapes are represented as super-quadrics (SQs) (see Cleary, 2004 for details). The shape of a super-quadric particle is defined by

$$\left(\frac{x}{a}\right)^m + \left(\frac{y}{b}\right)^m + \left(\frac{z}{c}\right)^m = 1 \qquad (4)$$

The resultant particle shape is then somewhere between an ellipsoid and a brick with the angularity/smoothness of the corners controlled by the choice of m (with $m = 2$ being ellipsoidal and large m being a brick) and the aspect ratios being controlled by the ratios of the semi-major axes (b/a and c/a).

Blade Wear Calculation

The incremental blade wear is modelled in a series of sequential sub-simulation steps where each step is of duration t_w. In each step, the shear power absorbed by the blade surface due to particle collisions is calculated and then converted to a surface wear measure. This wear is then used to erode the blade surface. This process is repeated multiple times until the entire wear life is modelled. Cleary et al. (2010) used this approach to predict the shape evolution in a HICOM mill and further details of this modelling approach are also in Cleary and Owen (2015) and Franke et al. (2015).

The blade is represented by a surface mesh with triangular surface elements. A collision between particle p and surface mesh element E results in the following shear power being absorbed at the surface element

$$S_{pE} = v_t F_t. \qquad (5)$$

The wear is assumed to be frictional dominated and so the shear power intensity was used as a predictor. The total shear power absorbed by the element, S_E, is then the summation of S_{pE} for all particle collisions with element E over the duration t_w. The element wear is calculated using this absorbed shear power and a calibration constant α,

$$W_E = \alpha S_E. \qquad (6)$$

The calibration constant is used to convert the shear power absorbed at each element into a surface element wear W_E. In the simulations presented here the calibration constant α was chosen to give a maximum surface element wear of 0.25 mm over the first sub-simulation, giving $\alpha = 3.3 \times 10^{-6}$ m/W for this configuration.

The surface wear is mapped onto the nodes of the mesh using a linear interpolation ensuring existing geometric edges are accounted for in the interpolation process. The resulting nodal displacement at node i is then

$$dx_i = \sum_E \beta_{iE} W_E n_E \qquad (7)$$

where n_E is the element normal for surface element E and and β_{iE} is the weight used in mapping the surface element wear W_E to node i. After the nodes are displaced the surface mesh is corrected to ensure surface elements do not invert during the nodal displacement. This process is repeated for a pre-defined number of flow sub-simulations. In this study the sub-simulation duration t_w is equivalent to two full revolutions of the blade to ensure the shear energy absorption calculated at each element is statistically meaningful.

SIMULATION SETUP

The high shear mixer geometry is the same as used in Cleary and Sinnott (2008) and Sinnott and Cleary (2015). It consists of a vertical cylindrical bowl of diameter 135 mm with a flat, horizontal floor. The rectangular blade impeller used to perform the mixing is 7 mm high in the vertical direction and 2 mm thick. The rotation axis of the blade is vertical and located at the centre of the bowl. The blade length spans the diameter of the bowl with a small clearance gap between blade and walls and bottom of the blade and floor. The configuration is shown in Figure 1 and highlights the clearance dimension for the blade set up. The blade rotates counter-clockwise at 100 rpm which is equivalent to a tip speed of 0.71 m/s.
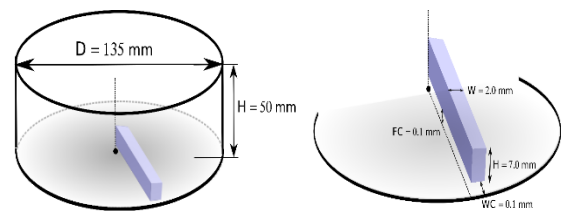

Figure 1: Schematic showing a) the blade mixer geometry, the blade/wall clearance (WC = 0.1 mm) and blade/floor clearances (FC = 0.1 mm).

For each simulation, the bowl was initially filled to a level height of 15 mm with SQ particles containing shape factors $2.5 < m < 6.0$ and major and intermediate aspect ratios $0.5 < a$, $b < 1.0$. The particle-particle and particle-boundary coefficients of restitution were chosen to be 0.9 representing a reasonably elastic material. A dynamic coefficient of friction of 0.4 was chosen for both particle-particle and particle-boundary interactions. Steady flow conditions were established prior to the commencement of the blade wear simulations by running the configuration for 0.5 revolutions of the blade first. Simulations with different

blade clearances of 0.1 mm and 0.3 mm were performed to understand the effect of the clearance size on the blade wear. Further simulations with two different particle size distributions (PSD) were also performed to investigate the sensitivity of blade damage to particle size. The details for each case are summarised in Table 1.

Case	PSD (mm)	Clearance (mm)	# particles
Base	0.45 - 0.55	0.1	914,000
2	0.45 - 0.55	0.3	914,000
3	1.45 - 1.55	0.1	62,000

Table 1: Details of the different simulation cases performed for this study.

Each simulation was performed as a sequence of eight sub-simulations covering the lifespan of the blade with its geometry being modified according to the wear distribution predicted in the previous sub-simulation. No erosion of the mixing bowl surfaces was included in the model since these are much lower than for the blade.

RESULTS

Particulate flow pattern in the mixer

The steady flow pattern for the base case (0.5 mm particles with a blade clearance of 0.1 mm) is shown in Figure 2 with particles coloured by radial, tangential and axial velocities respectively in order to characterise the nature of the flow over the blade and therefore the abrasive environment that the blade moves through. Particles pushed in front of the blade bank up and form a heap. The heap is located at a large radial distance from the centre of the mixing bowl and therefore the bed weight and the pressure on the blade increases with radial distance. Particles on the heap surface, and in front of the blade, flow radially outwards towards the cylindrical wall of the container. Conversely, particles behind the blade flow radially inward. Particles inside the heap load the front face of the blade and then flow up and over the blade leading to abrasion of the blade surface. A void forms behind the tip of the blade which largely protects the rear face of the blade from erosion. In the next section we examine how the resulting radial/vertical circulation flow structures influence the erosion of the blade geometry.

### Blade erosion for 0.1 mm clearance (Base Case)

In this section we examine the incremental erosion of the blade in response to the abrasive flow environment introduced in the previous section for the base case. We note that at this point in time we are unable to validate our wear results due to the lack of experimental data for this configuration. Cleary, Owen et. al (2010) used this approach to predict the shape evolution in a HICOM mill and achieved good agreement with the measured worn liner profile.
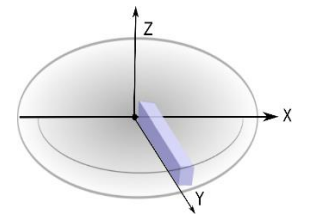
(a) Radial velocities
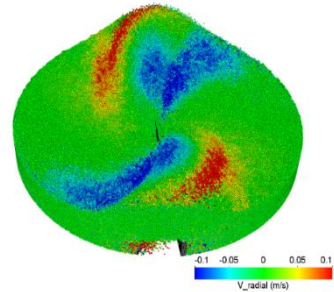
(b) Tangential velocities
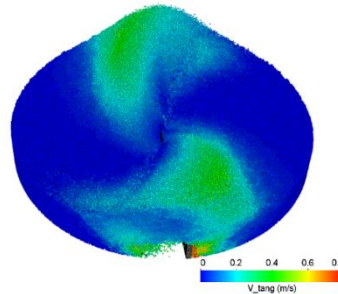
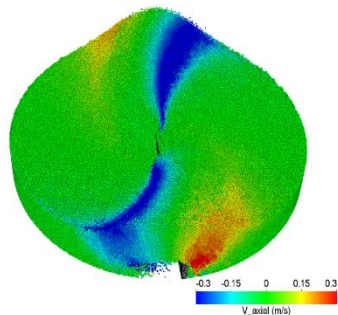**(c) Vertical velocities**

Figure 2: Steady flow pattern for the base case (0.5 mm particles with a blade clearance of 0.1 mm) using an unworn blade impeller. Particles are coloured by a) radial velocities; b) tangential velocities; and c) vertical/axial velocities.

Figures 3a&b show an edge-on and top view of the blade respectively. The geometry at 25%, 50%, 75% and 100% of the maximum lifespan of the blade is shown. At 25% of the maximum lifespan, there is initial erosion of the top and bottom edges of the tip of the blade. By 50% of the maximum lifespan, a clear radial damage distribution of the top edge is evident with more material lost close to the tip and the blade tip rounding. The radial dependence of the blade erosion continues for the 75% and 100% profiles resulting in a very thin worn tip which is about 40% of the unworn blade thickness. There is also a vertical dependence to the worn profile. The top half of the blade erodes at a greater rate than the bottom half due to the flow up and over the top of the blade.
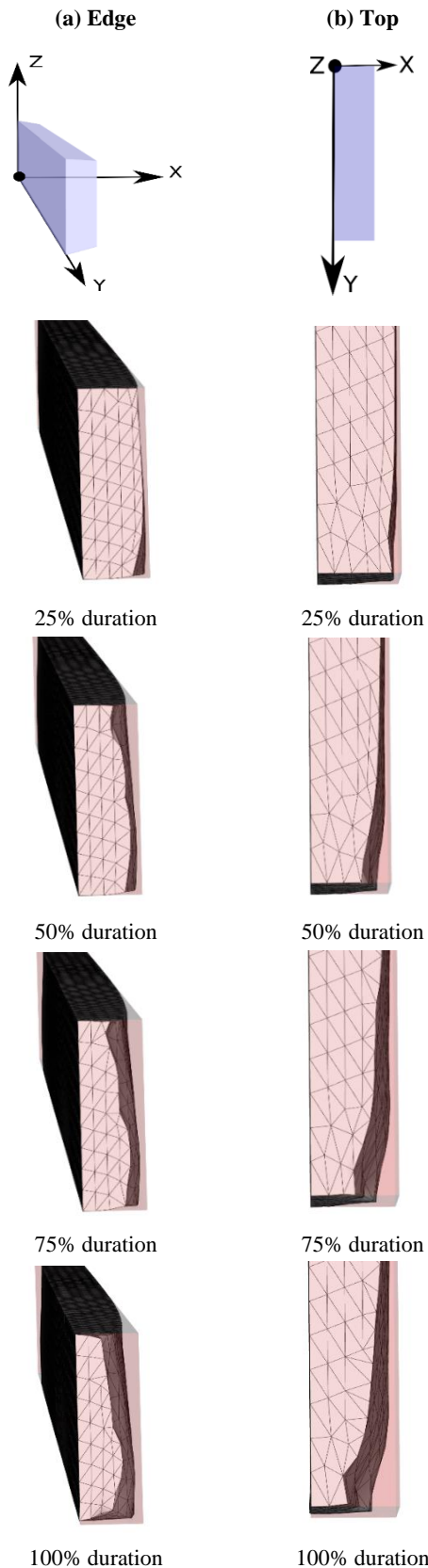
(a) Edge **(b) Top**

25% duration 25% duration

50% duration 50% duration

75% duration 75% duration

100% duration 100% duration

Figure 3: Progressively worn blade profiles at 25%, 50%, 75% and 100% of the maximum lifespan for the base case. The original unworn blade is shown as the transparent region. An edge view (a) and top view (b) of the blade highlight the 3D erosion of the blade tip.

Blade erosion for 0.3 mm clearance (Case 2)

An increase in the clearance gap between blade and wall leads to differences in the distribution of wear of the blade tip. Figure 4 compares the fully eroded blade state for clearances of 0.1 mm and 0.3 mm.
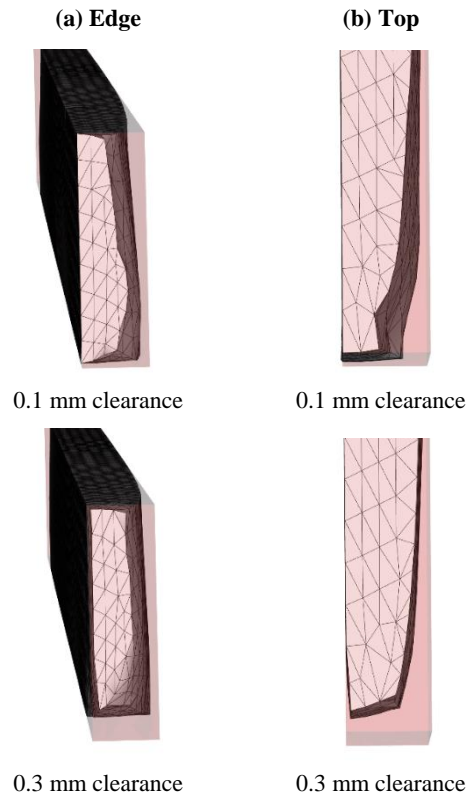
(a) Edge **(b) Top**

0.1 mm clearance 0.1 mm clearance

0.3 mm clearance 0.3 mm clearance

Figure 4: The fully worn blade profile shown for a) edge and b) top views for a blade/wall and blade/floor clearance of 0.1 mm and 0.3 mm.

Increasing the gaps between the blade tip and the wall and between the floor and the bottom of the blade increases the likelihood of flatter particles being caught inside the gaps. A clearance of 0.3 mm is sufficiently large to allow flat particles with an aspect ratio of 0.5 into the gaps. When this occurs, the rate of abrasive wear increases dramatically as constrained particles inside the gaps are dragged around by the blade resulting in scouring of the end and bottom faces of the blade tip. This leads to preferential rounding of both the bottom edge of the blade and the vertical leading edge of the blade tip. The blade length becomes shorter over time (so that the clearance becomes larger) allowing greater particle flow into the gaps. This modifies the rate of wear so that it is non-linear over the lifespan of the blade.

Figure 5 shows a cross-sectional slice of the blade at a radial distance 65 mm from the axis of rotation (near the blade tip). The progressive erosion of the front face of the blade is evident for both 0.1 mm and 0.3 mm clearance gap cases. Results of the 0.1 mm case show the upper half of the front face erodes preferentially. This is in contrast to the 0.3 mm case which shows a more uniform erosion of the front face. The larger clearance also leads to significant erosion of the bottom of the blade. The wear rate of the bottom of the blade is non-linear. The rate increases after 25% of the maximum lifespan as the gap widens sufficiently for greater particle flow into the gap. It then reduces again after 75% of the lifespan once the gap can include more than one particle layer beneath the blade.

This demonstrates that very large differences in the wear distribution can arise based solely on increasing the size of the clearance to match the minor axis dimension of the non-spherical particles. This will be a real process issue for any rotary mixing devices that rely on impeller/wall clearances comparable in size to the particles being processed. For example, the choice of clearance size between floor and bottom of the blade is a compromise between minimising the number of stagnant, non-mixed particle layers at the bottom of the bowl versus subjecting the paddle to a significant abrasive wear environment.

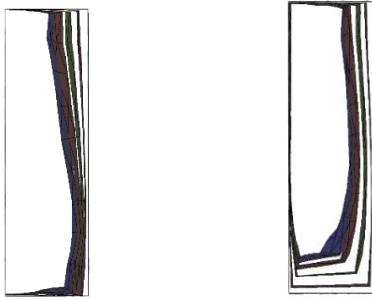**(a) 0.1 mm clearance**   **(b) 0.3 mm clearance**

Figure 5: Cross-sectional view of the blade at radial distance 65 mm from the rotation axis for a) 0.1 mm and b) 0.3 mm clearance cases. Profiles at 25%, 50%, 75% and 100% lifespan are shown.

Effect of particle size (Case 3)

Figure 6 shows the differences in flow over the blade tip for 0.5 mm and 1.5 mm particles with a clearance gap of 0.1 mm in both cases. The bed dynamics in front of the blade modestly change with particle size. For the coarse particles, there is a single packed particle layer (orange/red) pressed against the front of the blade which tends to shield the upper leading edge of the blade from particles flowing over it. In contrast, the bed of smaller particles results in multiple layers of tightly packed particles banking up in front of the blade. This results in a much smoother flow field with more interaction between particles and the upper leading edge of the blade. Also, particles well in advance of the blade are accelerated via chains of point-to-point contacts which extend over a much larger distance in front of the blade than for the coarser particle sizes. This mobilises multiple particle layers far in front of the blade to migrate upwards and over the blade.

The flow is therefore sensitive to the number of packed particle layers in the bed (or the coarseness of the particle size relative to the blade height). Since the flow pattern over the blade influences wear, it is therefore reasonable to expect that the details of wear may depend on particle size.

The bed pressures and surface speed of particles sliding over the blade surface contribute to the shear power (abrasive energy loss) absorbed by the blade surface. Figure 7 shows the distribution of the surface speed, pressure, and shear energy absorption for the 0.5 mm and 1.5 mm particle size cases at 25% of the wear duration for both cases. The surface speed is more uniform over the front face of the blade for the 1.5 mm particles whereas surface speeds are greater around the upper leading edge of the blade for the 0.5 mm particles. The 0.5 mm particles pack more tightly at the leading face in a pile that is about ¾ the height of the blade (see Figure 6) and is pushed around by the blade.

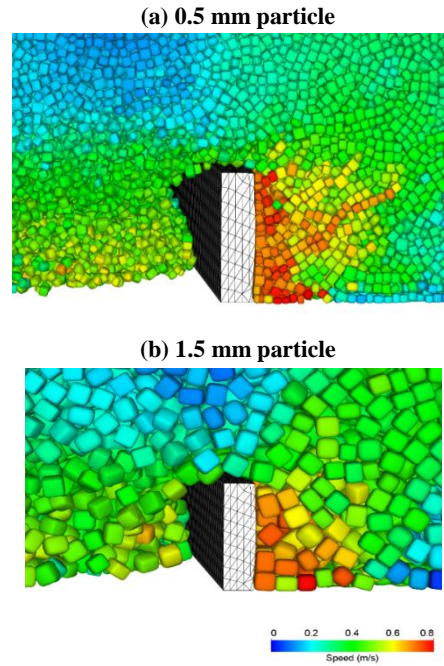**(a) 0.5 mm particle**

(b) 1.5 mm particle

Figure 6: Close-up of flow over the blade tip for a) 0.5 mm and b) 1.5 mm particles for a clearance of 0.1 mm.
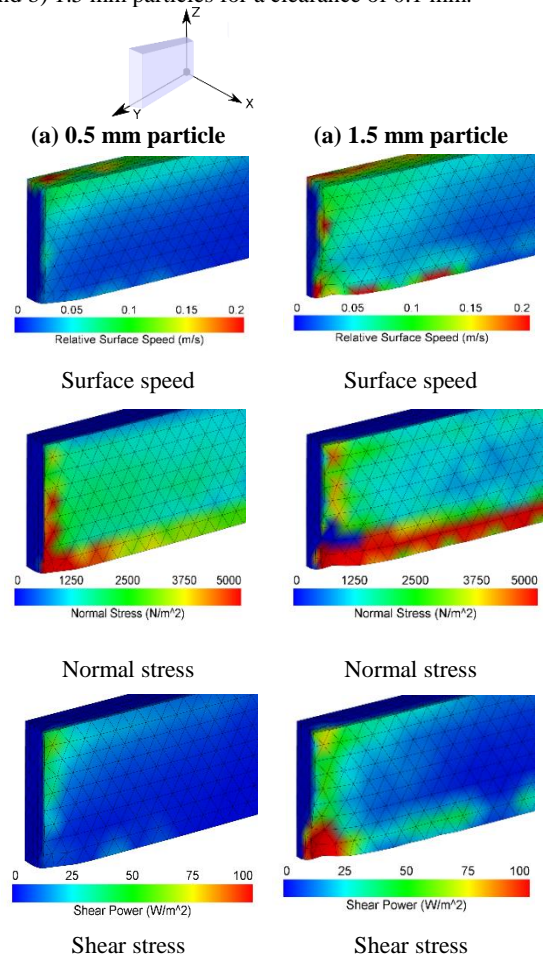

Figure 7: Worn blade profile at 25% of the maximum lifespan for (a) 0.5 mm particles (left) and (b) 1.5 mm particles (right). The mesh is coloured by (i) relative surface speed of the particles; (ii) pressure exerted onto the blade; and (iii) shear energy losses absorbed by the blade.

Therefore there is very little relative movement between the particles and the blade front face. In contrast there is only 1-2 particle layers for the 1.5 mm particles in front of the blade which results in substantial velocity fluctuations between particles and blade surface. Bed pressures exerted onto the front face of the blade appear mostly independent of particle size except for high pressures experienced along the bottom leading edge of the blade tip for the 1.5 mm particles. The combination of high pressures along the bottom leading edge and sliding of larger particles across the lower leading corner of the blade tip results in substantial shear energy loss leading to significant erosion of the blade corner.

Figure 8 shows a comparison of the worn profile of the blade tip at 25% of the maximum lifespan for the two particle size cases. Edge and top views are shown. The 1.5 mm particles cause significant abrasive scouring of the bottom leading corner of the blade tip compared to the 0.5 mm particle size case. However, the top half of the blade erodes similarly for both particle size cases with slightly more erosion occurring at the top leading corner of the blade for the 1.5 mm particle case.
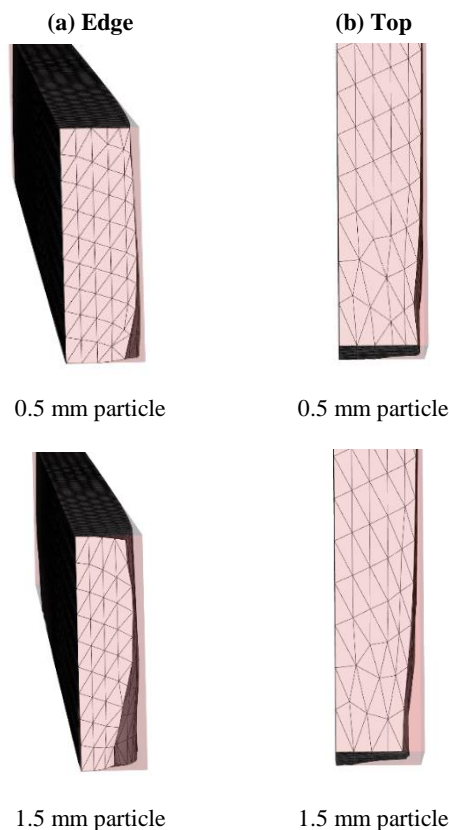
(a) Edge **(b) Top**

0.5 mm particle   0.5 mm particle

1.5 mm particle   1.5 mm particle

Figure 8: Comparison of the worn blade profile at 25% of the lifespan for the 0.5 mm particles and 1.5 mm particles. An edge view (a) and top view (b) of the blade highlight the 3D erosion of the blade tip for each case.

CONCLUSION

We have examined the erosion of the blade in DEM simulations of a high shear mixer. Specifically the effect of blade clearance and particle size on the eroded profile was studied. It was found that the blade clearance can have a significant non-linear effect on the worn blade profile. Larger clearances lead to preferential rounding of the edges of the blade as particles become dragged into the clearance,

which in turn increases the rate of abrasive wear of the blade tip. Increasing particle size results in higher particle surface speeds and pressures on the leading bottom edge of the blade. These in turn lead to increased erosion of the lower corner of the blade. Future work will examine the effect of blade erosion on the mixing performance of this configuration.

REFERENCES

CLEARY, P.W., OWEN, P.J., HOYER, D.I., and MARSHALL, S. (2010), "Effect of liner design on performance of a HICOM® mill over the predicted liner life cycle", *Int. J. Mineral Processing* **134**, 11-22.

CLEARY, P.W., and OWEN, P.J., (2015), "Prediction of mill liner shape evolution and changing operational performance during the liner life cycle: Case study of a Hicom mill", *Int. J. Numer. Meth. Eng.* **81**, 1157-1179.

CLEARY, P.W., and SINNOTT, M.D., (2003), "3D DEM Simulations of High Shear Mixers", *Third International Conference on CFD in the Minerals and Process Industries,* Melbourne, Australia, 10-12 December 2003.

CLEARY, P.W., and SINNOTT, M.D., (2008), "Assessing mixing characteristics of particle-mixing and granulation devices", *Particuology* **6**, 419-441.

CONWAY, S.L., LEKHAL, A., KHINAST, J.G., and GLASSER, B.J., (2005), "Granular flow and segregation in a four-bladed mixer", *Chemical Engineering Science* **60**, 7091-7107.

FRANKE, J., CLEARY, P.W., and SINNOTT, M.D., (2015), "How to account for operating condition variability when predicting liner operating life with DEM − A case study", *Minerals Engineering* **73**, 53-68.

JUREVICIUS, J., SIVILEVICIUS H., and SPRUOGIS B., (2003), "Analysis of wearing-out causes for revolving-blade mixers and their reliability improvement", *Transport* **XVIII**, 40-48.

LEKHAL, A., GIRARD, K.P., BROWN, M.A. KIANG, S., and KHINAST, J,G, (2003), "Impact of agitated drying on crystal morphology:KCl-water system", *Powder Technology* **132**, 119-130.

LITSTER, J.D., (2003), "Scaleup of wet granulation processes: science not art", *Powder Technology* **130**, 35-40.

REMY, B., KHINAST, J.G., and GLASSER, B.J., (2009), "Discrete element simulation of free flowing grains in a four bladed mixer", *AIChE Journal 55* **8**, 2035-2048.

SARKAR A., and WASSGREN. C.R., (2009), "Simulation of a continuous granular mixer:Effect of operating conditions on flow and mixing", *Chemical Engineering Science* **64**, 2672-2682.

SINNOTT, M.D., and CLEARY, P.W., (2015), "The Effect of Particle Shape on Mixing in a High Shear Mixer", *Journal Comp. Particle Methods*, DOI: 10.1007/s40571-015-0065-4.

ZHOU, Y.C., YU, A.B., STEWART, R.L., and BRIDGEWATER, J., (2004), "Microdynamic analysis of the particle flow in a cylindrical bladed mixer", *Chemical Engineering Science* **59,** 1343-1364.